Benzothiadiazole-triphenylamine as an efficient exciton blocking layer in small molecule based organic solar cells

Peer-reviewed author version

Calio, Laura; Patil, Bhushan R.; Benduhn, Johannes; VANDEWAL, Koen; Rubahn, Horst-Guenter; Madsen, Morten; Kazim, Samrana & Ahmad, Shahzada (2018)
Benzothiadiazole-triphenylamine as an efficient exciton blocking layer in small molecule based organic solar cells. In: SUSTAINABLE ENERGY & FUELS, 2(10), p. 2296-2302.

DOI: 10.1039/c8se00251g
Handle: http://hdl.handle.net/1942/27868

Benzothiadiazole-triphenylamine as efficient exciton blocking layer in small molecule based organic solar cells

Received 00th January 20xx,
Accepted 00th January 20xx

DOI: 10.1039/x0xx00000x

www.rsc.org/

Laura Caliò,[a] Bhushan R. Patil,[d] Johannes Benduhn,[e] Koen Vandewal,[e,f] Horst-Günter Rubahn[d], Morten Madsen,[d] Samrana Kazim[a,b] and Shahzada Ahmad[a,b,c]

We have designed a small molecule based on BTD-TPA_2, which is an electron-poor benzothiadiazole core with two electron-rich triphenylamine arms. BTD-TPA_2 was synthesized in a facile manner using Suzuki cross-coupling reaction. The molecule was rationally designed to take advantage from the synergetic effect of BTD, which allows formation of a favorable band gap material, while triphenylamine (TPA) moieties will favour efficient hole extraction and transport properties. A thin layer of BTD-TPA_2 was inserted in between the photo-active DBP/C_{70} layer stack and the MoO_x electrical contact. With an optimized interlayer thickness of 35 nm, the attained photovoltaic (PV) properties were substantially higher than those of the reference devices. This has its origin in BTD-TPA_2's dual functionality i.e. efficient exciton blocking and improved hole extraction at the anode contact. The obtained results led to an improved power conversion efficiencey of 5.66% for a vacuum deposited bilayer DBP/C_{70} solar cell, which will be new state-of-the-art for bilayer DBP based solar cells.

Introduction

Organic solar cells (OSCs) have been intensively investigated over the last decades with the aim to further optimize their photovoltaic (PV) performance, currently yielding power conversion efficiency (PCE) value of up to 15%[1]. OSCs represent a competitive edge due to their intriguing features such as low material and fabrication costs[2,3], exemplified by roll-to-roll (R2R) processing techniques[4,5], along with the possibility to develop thin, aesthetic, flexible, transparent and portable solar modules[6–9] as compared to other thin film PV technology. Diverse device architectures have been investigated so far, such as donor and acceptor (D-A) bilayer (planar heterojunction, PHJ) and bulk heterojunction (BHJ) structures, in conjunction with innovative materials, such as polymeric semiconductors and small organic molecules as donor and acceptor materials. Small organic molecules possess numerous benefits, such as high purity, easy processability and low batch-to-batch variation in performance, this allows to explore a large number of novel materials to be employed as donor and acceptor molecules in OSCs[10,11]. Tetraphenyldibenzoperiflanthene (DBP) as the donor and C_{70} as the acceptor material, have been well investigated and employed in both efficient bulk[12] and bilayer[13,14] heterojunction OSCs configurations. DBP is a well-known small organic conjugated material, and was extensively used in opto-electrical devices, and OSCs in particularly[15–17]. The main advantages of DBP as donor material in OSCs is it's high optical absorption and relatively deep lying highest occupied molecular orbital (HOMO) level (-5.5 eV [18]), which was found to be ideal for efficient exciton splitting at the DBP/fullerene interface, while maintaining relatively high open circuit voltages (V_{OC}) [13,19]. DBP has a strong absorption in the visible region from 300 - 700 nm, with a peak absorption coefficient of 4.2×10^5 cm^{-1} at λ = 610 nm, a relatively high hole mobility of ~10^{-4} $cm^2/(V\cdot s)$[19], and an exciton diffusion length of up to 16±1 nm, as reported by Bergemann et al.[20]. DBP based devices employing MoO_x as hole extraction layers were found to yield decent performance, though excitons were not blocked at the DBP/MoO_x interface, but were quenched.[21] A possible strategy for overcoming exciton quenching effects is to introduce an exciton blocking layer (EBL), which can prevent excitons to leave the active layer, and increases the possibility for dissociation at the D-A interface[19]. Zhang et al. have reported the use of three well-known small organic hole transporting materials (HTM), such as 5,10,15-tribenzyl-5H-diindolo[3,2-a:3',2'-c]-carbazole (TBDI), *N,N'*-diphenyl-*N,N'*-bis(1-naphthyl)-1,1'-biphenyl-4,4'-diamine (NPB) and 1,1'-bis(di-4-tolylaminophenyl)cyclohexane (TAPC), to serve as EBLs in DBP based planar hetero-junction cells[22]. It was reported that the HTMs successfully blocked excitons at the donor/hole extraction interface, yielding a PCE of 1.70%, 1.33%, and 1.33%, respectively, whereas the control device without any EBL gave a PCE of 1.25%. Patil et al.[14] have recently reported an analogous study in which a ultra-thin layer of *N,N'*-di-1-naphthalenyl-*N,N'*-diphenyl [1,1':4',1'':4'',1'''-quaterphenyl]-4,4'''-diamine (4P-NPD) was efficiently used as EBL in DBP/C_{70} inverted planar heterojunction solar cells, achieving a PCE of 3.69% for the optimized EBL thickness versus a PCE of 2.97% for the EBL-free reference cells. In this work, we have introduced BTD-TPA_2 as an EBL sandwiched between the electron donor and hole transporting layer in a classical planar hetero-junction solar cells, and demonstrate its dual functionality i.e. efficient exciton blocking and improved hole extraction at the anode contact and electron co-donor. The obtained results led to an improvement in PCE values, and an impressive 5.66% for bilayer DBP/C_{70} solar cells was obtained with an optimized EBL thickness of 35 nm(15mM BTD-TPA_2), and is among the highest reported PCEs to date for bilayer DBP based solar cells.

[a] *Abengoa Research, Abengoa, C/ Energía Solar nº 1, Campus Palmas Altas-41014, Sevilla, Spain.*
[b] *BCMaterials, Basque Center for Materials, Applications and Nanostructures, UPV/EHU Science Park, 48940 Leioa, Spain*
Tel: +34 946128811 Email:shahzada.ahmad@bcmaterials.net
[c] *IKERBASQUE, Basque Foundation for Science, Bilbao, 48013, Spain*
[d] *SDU NanoSYD, Mads Clausen Institute, University of Southern Denmark, Alsion 2, 6400 Sønderborg, Denmark*
[e] *Dresden Integrated Center for Applied Physics and Photonic Materials (IAPP) and Institute for Applied Physics, Technische Universität Dresden, Nöthnitzer Str. 61, 01187 Dresden, Germany*
[f] *Current address: IMO-IMOMEC, Hasselt University Wetenschapspark 1, 3590 Diepenbeek, Belgium*

† Footnotes relating to the title and/or authors should appear here.
Electronic Supplementary Information (ESI) available: [details of any supplementary information available should be included here]. See DOI: 10.1039/x0xx00000x

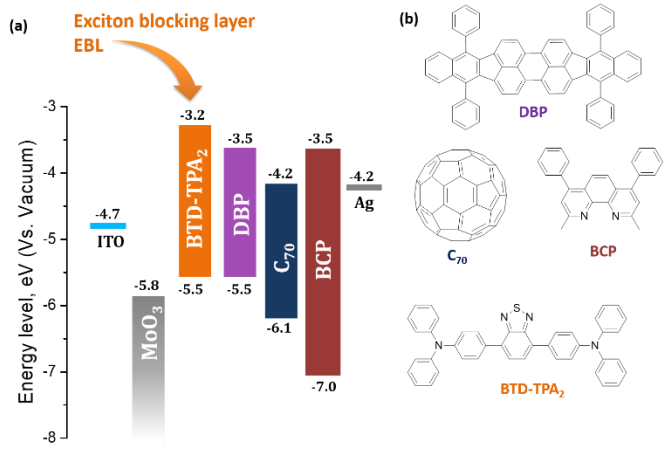

Figure 1. a) Band alignment and b) molecular structure of the materials used in this study.

Results and discussion

Figure 1, represents the the architecture of the devices studied in this work along with the molecular structure of the materials used. MoO_x was employed as hole transporting layer in the OSCs, due to its efficient and stable hole extraction capabilities[23,24]. A thin layer of 2,9-dimethy-4,7-diphenyl-1,10-phenathroline (bathocuproine, BCP) was used as electron transporting material and hole blocking layer at the interface between the acceptor C_{70} and Ag cathode. BCP is a wide band gap electron transporting material, which also acts as a physical barrier in order to prevent damage to the active organic layer by the metal deposition. In a report, the Ag metal:BCP hybrid complex formed upon Ag evaporation, possess favorable states (LUMO level of the complex) inside the bandgap of BCP, leading to efficientelectron extraction in such cells[25]. In the past benzothiadiazole (BTD) based polymers and small molecules have been widely employed in opto-electrical devices, such as organic light emitting diodes (OLEDs) due to its fluorescent properties[26,27], while the development of D-A structures in combination with triphenylamine (TPA) moieties have been extensively employed as dye/active materials in dye sensitized solar cells (DSSC)[28,29]/OSCs[30,31]. $BTD\text{-}TPA_2$ is a small organic molecule, having an electron-poor benzothiadiazole core with two electron-rich triphenylamine arms, and has been explored as red-light-emitting material in OLED application[32,33].

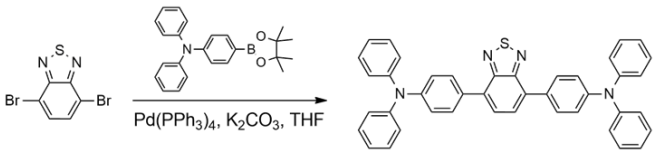

Scheme 1. Synthetic route adopted for the synthesis of $BTD\text{-}TPA_2$.

$BTD\text{-}TPA_2$ was synthesized in a facile manner using a Suzuki cross-coupling reaction (scheme 1). The presence of triphenylamine moieties provides an amorphous thin film with efficient hole transport properties, while the presence of the BTD core lead to the suitable frontier orbital energy matching with the donor HOMO[34]. Differential scanning calorimetry (DSC), thermogravimetric analysis (TGA) curves and cyclovoltammetry (CV) measurements are reported in Fig. S2 (Supporting Information), showing a HOMO level of -5.54 eV and a LUMO level of -3.24 eV is higher than the LUMO level of DBP, allowing the use of $BTD\text{-}TPA_2$ as exciton blocking material and potential donor in such devices. (chemical structure and band alignment are shown in Figure 1).

To optimize the thickness of the films, varying concentrations (eight different samples) of $BTD\text{-}TPA_2$ were prepared in chlorobenzene, and were spin-coated (under similar conditions) to form an interfacial layer between the thermally evaporated layers of MoO_X and DBP (structure depicted in Figure 1). The concentrations of $BTD\text{-}TPA_2$ were chosen as such to allow for the formation of low layer thickness and was in the range of 40 mM to 1.25 mM (corresponding to a thickness between 65 nm and 15 nm). For comparative purposes, reference devices (without EBL, labelled as 0 mM) were fabricated. The devices present the following structure: ITO/$BTD\text{-}TPA_2$ (0-40 mM)/DBP (20 nm)/C_{70} (30 nm)/BCP (10 nm)/Ag (100 nm).
The employment of $BTD\text{-}TPA_2$ as EBL showed notable enhancements in the PV performance of the devices, as shown in Table 1, while statistical values reported in Table S1 (Supporting Information).

Table 1. Summary of PV parameters of the best performing OSCs employing EBL layers of $BTD\text{-}TPA_2$ deposited from chlorobenzene using different concentrations. Devices structure: ITO/$BTD\text{-}TPA_2$ (0-65 nm)/DBP (20 nm)/C_{70} (30 nm)/BCP (10 nm)/Ag (100 nm).

Concentration/ thickness $BTD\text{-}TPA_2$	V_{OC} (mV)	J_{SC} (mA/cm²)	FF (%)	PCE (%)
40 mM/65 nm	870	6.81	39.00	2.32
30 mM/45 nm	940	7.86	46.71	3.14
20 mM/40 nm	940	8.84	54.56	4.56
15 mM/35 nm	950	9.53	62.73	5.66
10 mM/30 nm	940	9.66	56.38	5.13
5 mM/25 nm	950	7.69	63.42	4.62
2.5 mM/20 nm	950	7.34	61.88	4.31
1.25 mM/15 nm	860	6.56	68.92	3.88
0 mM/ 0 nm	900	6.69	64.86	3.91

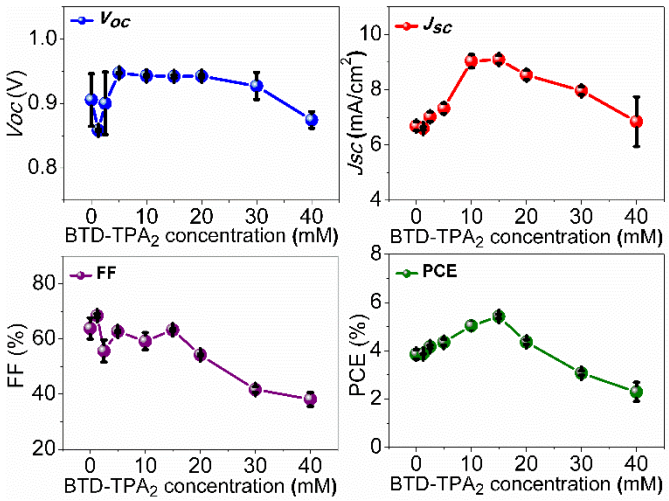

Figure 2. Summary of the photovoltaic parameters obtained with respect to BTD-TPA_2 concentration.

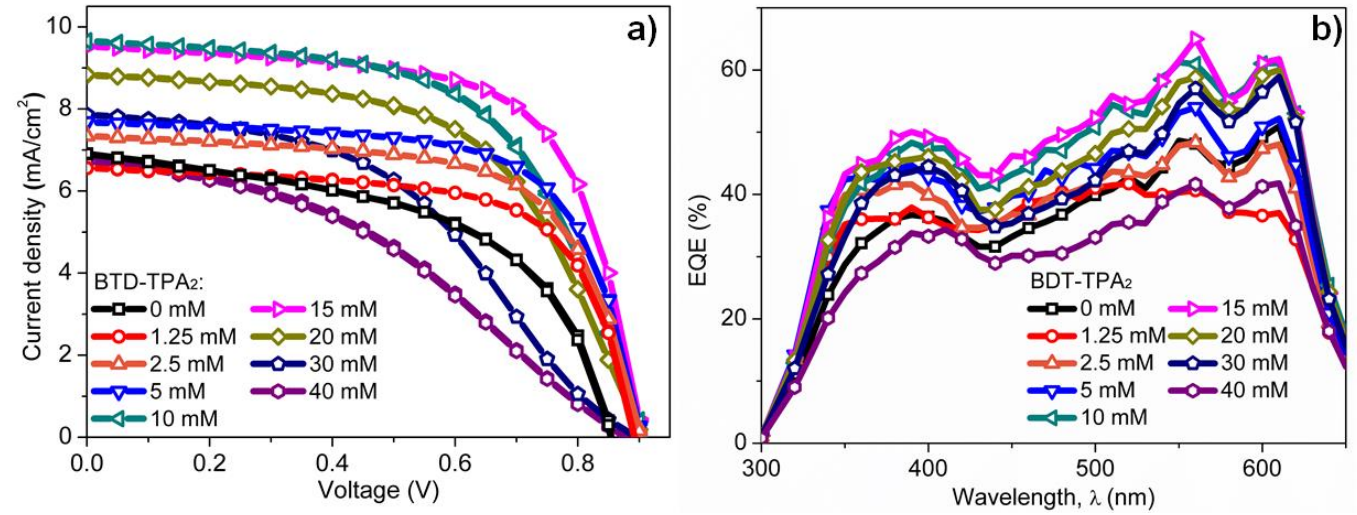

Figure 3. a) *J-V* characteristics and b) EQE measurements of OSCs fabricated with BTD-TPA_2 exciton blocking layers deposited from solution at different concentrations.

Enhancement in the short-circuit current density (J_{SC}) were obtained for all the devices encompassing of BTD-TPA_2 EBL, and the current density value obtained for the optimal concentrations of BTD-TPA_2 (which correspond to 15 and 10 mM, and to a thickness of 35 and 30 nm, respectively) was nearly 45% higher than the J_{SC} of the reference devices, i.e. an increment was obsevredrom 6.7 mA/cm^2 for the EBL-free reference devices to 9.5 mA/cm^2 for the best BDT-TPA_2-containing devices. Thus, the enhancement in the photocurrent indicates the effectiveness of the exciton-blocking properties of the BDT-TPA_2. The trend of the results obtained for the different BDT-TPA_2 concentrations is distinct, as seen from Figure 2 (PV parameter plots) and Figure 3a (*J-V* curves). The PV behaviour obtained from the thinnest EBL (1.25 mM solution, corresponding to a 15 nm thick layer) shows no significant improvement, yielding an V_{OC} of 860 mV, J_{SC} of 6.56 mA/cm^2, Fill Factor (FF) of 68.92% with an overall PCE of 3.88%, which are on par with the reference devices (PCE of 3.91%). By increasing the concentration and thus thickness, i.e. to 2.5 mM and 5 mM (20 and 25 nm thick layers, respectively), a modest increase of the current density was observed due to the exciton blocking behavior of BTD-TPA_2, with a J_{SC} of 6.69 mA/cm^2 for the reference device to 7.34 mA/cm^2 and 7.69 mA/cm^2 of the devices prepared with BTD-TPA_2 at 2.5 mM and 5 mM, respectively. The significant enhancements were obtained with the devices containing the EBL deposited from the solution at 10 and 15 mM concentrations, gave an impressive overall PCE of 5.13% and 5.66%, respectively, which corresponds to an enhancement of over 45% with respect to the reference devices. Notably, by further increasing the concentration, to 20, 30 and 40 mM (i.e. to 40, 45 and 65 nm), a reverse trend was obtained, and resulted in lower device performance, i.e. PCE of 4.56%, 3.14% and 2.32%, respectively. V_{OC} remains rather constant for most of the different concentrations, though an increase of 40-50 mV for devices including the BTD-TPA_2 layers (between 2.5 mM to 30 mM) was recorded. A drop in FF was obtained, in case of thicker layers, deposited from 30 and 40 mM

concentration. This we assigned to enhancement in series resistance caused by hampering of hole transport through the thicker EBL layer. These trends are also in accordance with the EQE measurements (Figure 3b). The maximum light harvesting abilities was attributed to the defined optimum concentration of BTD-TPA_2, i.e. 10-15 mM, showing a maximum conversion of over 60% in the 550-650 nm range, which corresponds to the peak of DBP absorption, whereas an almost constant increment in the EQE spectrum was observed over the range of 300-650 nm. We note that a co-donor effect may take place, allowing excitons generated in the BTD-TPA_2 layer (absorbing at shorter wavelengths as compared to DBP) to be dissociated into free carriers. From the registered EQE curves, the integrated value of J_{SC} was extracted for each configuration and are listed in Table S2. The integrated current density was consistent with the average values of current density registered by the *J-V* measurements (Table S2). The thickness of the EBLs at different concentrations was measured with the help of atomic force microscopy (AFM). The average values from the measurement of each film deposited on top of 10 nm of thermally evaporated MoO_x are listed in Table S3. The measured thickness was between 15 nm (1.25 mM) to 65 nm (40 mM). The best PV behavior was obtained from the deposition of 30-35 nm BTD-TPA_2 as EBL, corresponding to a concentration of 10-15 mM. Figure 4a shows the UV-vis absorption spectra for BTD-TPA_2 layers deposited from the different concentrated solutions sandwiched between the thermally evaporated MoO_x and DBP layers. As expected, with the increase of concentration (and therefore the thickness of BTD-TPA_2 layers), the absorption in the range of 400-500 nm and 300-350 nm sequentially increases, which corresponds to the absorption of the synthesized molecules, as shown in Figure 4a (black dotted line). Additionally, with the increase in the thickness of the EBL, a small reduction in the absorption of the peak at 610 nm was observed. As BTD-TPA_2 lacks absorbance in this range, we expect that this relatively small absorption change could occur due to changes in the orientation of the DBP molecules when deposited on top of BTD-TPA_2, as compared to on top of the MoO_x layer.

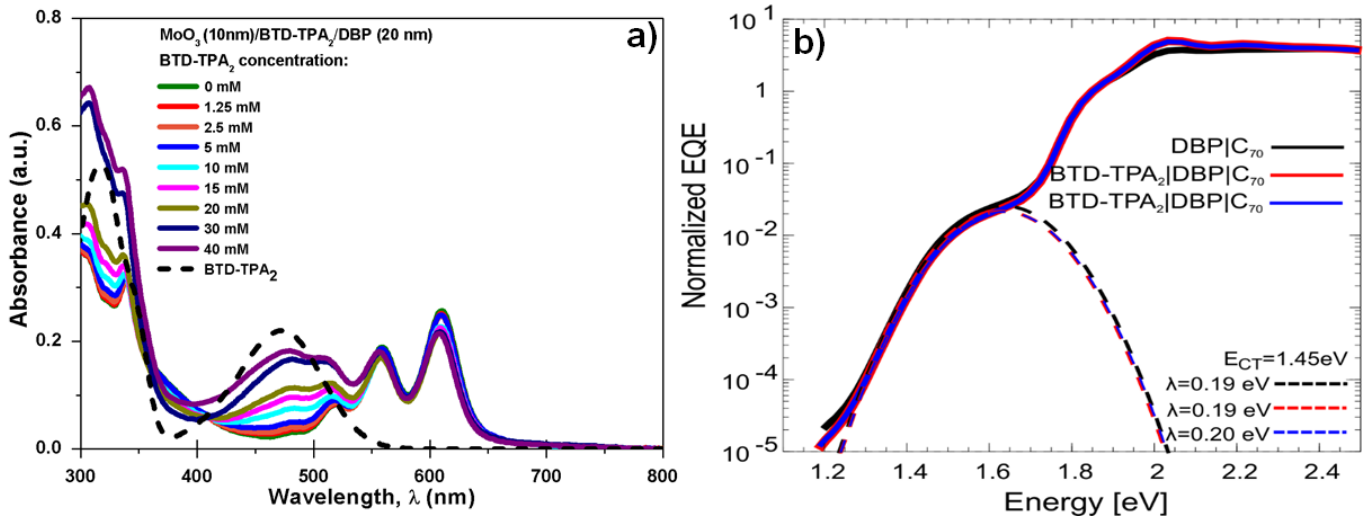

Figure 4. a) UV-Vis absorption spectra of the BTD-TPA_2 layers sandwiched between MoO_x and DBP layers (solid lines) and BTD-TPA_2 alone (dashed line) and b) sensitive-EQE measurements of the DBP/C_{70}-based reference device (black line) and two devices with BTD-TPA_2 using the best concentration (15 mM, red and blue lines) are shown.

Due to the relatively strong absorption of BTD-TPA_2 in the 400-550 nm range, which is complementary to the DBP main absorption at 550-650 nm, its usage as single donor and as co-donor with DBP was evaluated. For this purpose, two different thicknesses were selected to be evaluated as donor layer, 40 nm and 35 nm, which corresponds to 20 mM and 15 mM solutions respectively, and were deposited by spin-coating in a similar condition. Similarly, in order to evaluate its behavior as DBP co-donor, the concentrations of BTD-TPA_2 (15 and 20 mM) were kept alike and were probed together with an ultra-thin layer of DBP (5nm). On one hand, it can be deducted from data (Fig. S3 and Table S4 in Supporting Information) that the donor properties of the BTD-TPA_2 are less appealing compared to the reference donor DBP, resulting in devices with a PCE of maximum 2.44% for BTD-TPA_2 with 40 nm thickness, while a PCE of 3.91% was obtained for the reference DBP device. On the other hand, the use of BTD-TPA_2 as co-donor with an ultrathin layer of DBP showed a slight improvement in device efficiency, especially for the devices with higher concentration of BTD-TPA_2, i.e. 20 mM, resulting in a J_{SC} of up to 8.01 mA/cm^2 and a PCE of up to 4.19%. No significant change in terms of V_{OC} was observed. These results suggest that the use of BTD-TPA_2 as donor with DBP is a less useful strategy as compared to its exciton blocking properties. However, when used as exciton blocking layer, the co-donor effect will also be present, depending on the thickness of the EBL layer (Figure S4). As slight variations in the DBP absorption and open-circuit voltage was detected, pointing towards a possible structural modified donor layer, sensitive external quantum efficiency measurements (sEQE) were conducted to elucidate if the integrated BTD-TPA_2 layer affects the interface energetics and the

properties of the charge-transfer (CT) states at the donor/acceptor interface in the solar cells. In Figure 4b, sEQE measurements of the DBP/C_{70}-based reference device (black line) for the configuration, i.e. with BTD-TPA_2 in the best concentration (15 mM, red and blue lines) are shown. The two devices with the same concentration of BTD-TPA_2 show an identical behavior. The signal at low photon energies around 1.5 eV originates from the weak absorption related to CT state between the C_{70} and DBP layers. From the sEQE measurements, the energy (E_{CT}) and the reorganization energy (λ) of the CT state were determined by fitting low energy part of the spectrum as described by Vandewal et al[35]. These parameters mainly determine the V_{OC}[36,37]. Since no difference for both E_{CT} and λ in the reference DBP/C_{70} device and the BTD-TPA_2/DBP/C_{70}-based devices was found, we conclude that the interface energetics of DBP/C_{70} remains unchanged with the use of BTD-TPA_2, suggesting that the main function of the layer is to provide efficient hole extraction and exciton blocking at anode, in addition to the small co-donor effect. Additionally, it suggests non-radiative voltage losses are reduced due to reduced non-radiative recombination at the hole contact and resulted in an increase V_{oc}.

To elucidate the effects of the implemented layers on the hole extraction properties in the cells, *J-V* measurements of hole only devices with the different thicknesses of the BTD-TPA_2 layers were conducted. The results from the hole only devices are shown in Figure 5a. In the developed configuration, holes were injected into the device through the Ag electrode and extracted out of the device at the ITO electrode. Devices with the thicker BTD-TPA_2 layer (40 mM) show the lowest extraction properties, corresponding to a lower current density, and are at par with the EBL-free devices. Devices with BTD-TPA_2 layers deposited from the 10-15 mM concentrations presented the highest hole extraction efficiencies, demonstrating that the hole contact improves with the introduction of BTD-TPA_2 layer (up to 15 mM), but it decreases again due to the increased series resistance, arises with the use of thicker layers (obtained using BTD-TPA_2 above 15 mM).

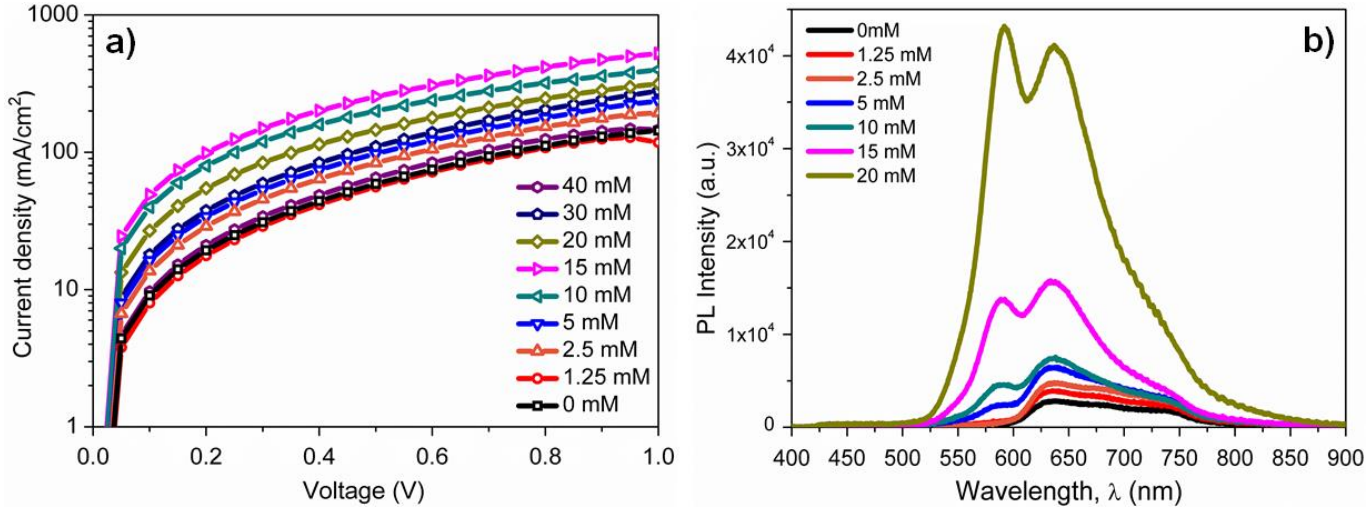

Figure 5. a) *J-V* characteristics of the hole only devices (HODs), fabricated with the architecture: ITO/MoO_x(10 nm)/BTD-TPA_2(different thickness)/DBP (20 nm)/Ag (100 nm); b) Photoluminescence measurements of the layer stack: Quartz/ MoO_x (10 nm)/BTD-TPA_2/ DBP (15 nm).

To illustrate the exciton blocking properties of BTD-TPA_2, photoluminescence (PL) measurements were made to compare the PL intensity of DBP using different concentrations of BTD-TPA_2. The excitation wavelength was centred between 330 nm and 380 nm. Figure 5b depicts that the PL intensity of DBP (600-800 nm) increases with an increased thickness of the BTD-TPA_2 layer and was found to be saturated for higher concentrations (30mM and 40mM) at a thickness of 45 and 60 nm respectively as shown in figure S7. With an increase in the thickness of BTD-TPA_2 layer, exciton quenching at the MoO_3 interface will be decreased, which leads to an increased PL intensity. This directly demonstrates its efficient exciton blocking capabilities by inhibiting charge recombination at the DBP donor and MoO_3 interface. We note that in addition to the DBP signal, a PL signal from the BTD-TPA_2 layers (centered at 585 nm) arises at a concentration of 5mM corresponds to the 25nm thickness.This PL signal furrther increases on increasing the BTD-TPA_2 layer thickness, and surpasses the intensity of the DBP main peak for concentrations above 15 mM. The enhancement in PL emission at 585 nm also indicates that BTD-TPA_2 participates simultaneously in the light absorption and exciton generation in the BTD layer and also proves its codonor effect.

Conclusions

We put forward small organic molecules based on BTD-TPA_2 , which was syntheiszed using simple Suzuki cross-coupling reaction and was employed as an effective exciton blocking material. The incorporation of BTD-TPA_2 significantly improve the photovoltaic performance of DBP/C_{70} based solar cells. By varying the concentration of the chlorobenzene solution from which BTD-TPA_2 was deposited, we have found that the optimal BTD-TPA_2 thickness for device integration was around 30-35 nm. Significant improvements in short-circuit current density were found, with an astonishing increment up to 45%, as compared to the J_{SC} of the

reference devices, i.e. increasing from 6.7 mA/cm^2 in the EBL-free reference devices to the 9.5 mA/cm^2 for the best BDT-TPA$_2$-containing devices. This resulted in an impressive PCE increase from 3.91% to 5.66%, which is the highest efficiency obtained to date in DBP based bilayer solar cells to the best of our knowledge. In order to elucidate the involved mechanisms, PL measurements were performed to confirm the exciton blocking properties of BTD-TPA$_2$, while hole-only devices reveal improved hole contact at low BTD-TPA$_2$ thickness, suggesting the ideal thickness of 30-35 nm. Additionally, sEQE measurements revealed no difference in the interface energetics at the DBP/C$_{70}$ interface upon EBL integration, suggesting that the integrated EBL only affects the hole extraction and exciton blocking properties at anode. This study put forward the design of BTD-TPA$_2$ molecules for its application as efficient exciton blocking materials in organic solar cells, to further push the device performances.

Conflicts of interest

There are no conflicts to declare.

Acknowledgements

This project has received funding from the European Union Seventh Framework Programme under grant agreement n° 607232 [THINFACE] and partially supported by European Research council grant [MOLEMAT, 72630], as well as by the German Federal Ministry for Education and Research (BMBF) through the InnoProfille project 'Organische p-i-n Bauelemente 2.2'.

Notes and references

1 X. Che, Y. Li, Y. Qu and S. R. Forrest, *Nat. Energy*, 2018, 422–427.

2 S. M. McAfee, S. V. Dayneko, P. Josse, P. Blanchard, C. Cabanetos and G. C. Welch, *Chem. Mater.*, 2017, **29**, 1309–1314.

3 T. T. Do, K. Rundel, Q. Gu, E. Gann, S. Manzhos, K. Feron, J. Bell, C. R. McNeill and P. Sonar, *New J. Chem.*, 2017, **41**, 2899–2909.

4 F. C. Krebs, S. A. Gevorgyan and J. Alstrup, *J. Mater. Chem.*, 2009, **19**, 5442.

5 X. Gu, Y. Zhou, K. Gu, T. Kurosawa, Y. Guo, Y. Li, H. Lin, B. C. Schroeder, H. Yan, F. Molina-Lopez, C. J. Tassone, C. Wang, S. C. B. Mannsfeld, H. Yan, D. Zhao, M. F. Toney and Z. Bao, *Adv. Energy Mater.*, 2017, **7**, 1–13.

6 Y. Galagan, J. E. J.m. Rubingh, R. Andriessen, C. C. Fan, P. W.m. Blom, S. C. Veenstra and J. M. Kroon, *Sol. Energy Mater. Sol. Cells*, 2011, **95**, 1339–1343.

7 M. Kaltenbrunner, M. S. White, E. D. Głowacki, T. Sekitani, T. Someya, N. S. Sariciftci and S. Bauer, *Nat. Commun.*, 2012, **3**, 770.

8 W. Wang, C. Yan, T. K. Lau, J. Wang, K. Liu, Y. Fan, X. Lu and X. Zhan, *Adv. Mater.*, 2017, **29**, 1–7.

9 J. Jean, A. Wang and V. Bulović, *Org. Electron. physics, Mater. Appl.*, 2016, **31**, 120–126.

10 F. C. Krebs, *Sol. Energy Mater. Sol. Cells*, 2009, **93**, 394–412.

11 N. Espinosa, R. García-Valverde, A. Urbina and F. C. Krebs, *Sol. Energy Mater. Sol. Cells*, 2011, **95**, 1293–1302.

12 X. Xiao, K. Lee and S. R. Forrest, *Appl. Phys. Lett.*, 2015, 213301.

13 M. Ahmadpour, Y. Liu, H. G. Rubahn and M. Madsen, *IEEE J. Photovoltaics*, 2017, **7**, 1319–1323.

14 B. R. Patil, Y. Liu, T. Qamar, H.-G. Ruban and M. Madsen, *J. Phys. D. Appl. Phys.*, 2017, **50**, 385002.

15 T. Kirchhuebel, M. Gruenewald, F. Sojka, S. Kera, F. Bussolotti, T. Ueba, N. Ueno, G. Rouillé, R. Forker and T. Fritz, *Langmuir*, 2016, **32**, 1981–1987.

16 S. Grob, A. N. Bartynski, A. Opitz, M. Gruber, F. Grassl, E. Meister, T. Linderl, U. Hörmann, C. Lorch, E. Moons, F. Schreiber, M. E. Thompson and W. Brütting, *J. Mater. Chem. A*, 2015, **3**, 15700–15709.

17 Z. Wang, D. Yokoyama, X.-F. Wang, Z. Hong, Y. Yang and J. Kido, *Energy Environ. Sci.*, 2013, **6**, 249–255.

18 D. Fujishima, H. Kanno, T. Kinoshita, E. Maruyama, M. Tanaka, M. Shirakawa and K. Shibata, *Sol. Energy Mater. Sol. Cells*, 2009, **93**, 1029–1032.

19 M. Hirade and C. Adachi, *Appl. Phys. Lett.*, 2011, **99**, 2012–2015.

20 K. J. Bergemann and S. R. Forrest, *Appl. Phys. Lett.*, 2011, **99**, 3–6.

21 X. Xiao, J. D. Zimmerman, B. E. Lassiter, K. J. Bergemann and S. R. Forrest, *Appl. Phys. Lett.*, 2013, **102**, 5–9.

22 J. Zhang, F. Yang, Y. Zheng, B. Wei, X. Zhang, J. Zhang, Z. Wang, W. Pu and C. Yang, *Appl. Surf. Sci.*, 2015, **357**, 1281–1288.

23 F. Wang, X. Qiao, T. Xiong and D. Ma, *Org. Electron. physics, Mater. Appl.*, 2008, **9**, 985–993.

24 D. Y. Kim, J. Subbiah, G. Sarasqueta, F. So, H. Ding, Irfan and Y. Gao, *Appl. Phys. Lett.*, 2009, **95**, 1–5.

25 H. Yoshida, *J. Phys. Chem. C*, 2015, **119**, 24459–24464.

26 K. M. Omer, S. Y. Ku, K. T. Wong and A. J. Bard, *J. Am. Chem. Soc.*, 2009, **131**, 10733–10741.

27 Y. Yang, Y. Zhou, Q. He, C. He, C. Yang, F. Bai and Y. Li, *J. Phys. Chem. B*, 2009, **113**, 7745–7752.

28 S. Somasundaram, S. Jeon and S. Park, *Macromol. Res.*, 2016, **24**, 226–234.

29 J. A. Mikroyannidis, P. Suresh, M. S. Roy and G. D. Sharma, *J. Power Sources*, 2010, **195**, 3002–3010.

30 D. Deng, Y. Yang, J. Zhang, C. He, M. Zhang, Z. G. Zhang, Z. Zhang and Y. Li, *Org. Electron. physics, Mater. Appl.*, 2011, **12**, 614–622.

31 H. Wang, Y. Liu, M. Li, H. Huang, H. M. Xu, R. J. Hong and H. Shen, *Optoelectron. Adv. Mater. Rapid Commun.*, 2010, **4**, 1166–1169.

32 T. Ishi-I, K. Ikeda, Y. Kichise and M. Ogawa, *Chem. - An Asian J.*, 2012, **7**, 1553–1557.

33 K. R. Justin Thomas, J. T. Lin, M. Velusamy, Y.-T. Tao and C.-H. Chuen, *Adv. Funct. Mater.*, 2004, **14**, 83–90.

34 C. Wang, Z. Cao, B. Zhao, P. Shen, X. Liu, H. Li, T. Shen and S. Tan, *Dye. Pigment.*, 2013, **98**, 464–470.

35 K. Vandewal, K. Tvingstedt, A. Gadisa, O. Inganäs and J. V.

Manca, *Phys. Rev. B - Condens. Matter Mater. Phys.*, 2010, **81**, 1–8.

36 K. Vandewal, K. Tvingstedt, A. Gadisa, O. Inganäs and J. V. Manca, *Nat. Mater.*, 2009, **8**, 904–909.

37 J. Benduhn, K. Tvingstedt, F. Piersimoni, S. Ullbrich, Y. Fan, M. Tropiano, K. A. McGarry, O. Zeika, M. K. Riede, C. J. Douglas, S. Barlow, S. R. Marder, D. Neher, D. Spoltore and K. Vandewal, *Nat. Energy*. 2017, **2**, 17053.